Upconversion Cross-Correlation Spectroscopy of a Sandwich Immunoassay

Lahtinen, Satu; Krause, Stefan; Arppe, Riikka Matleena ; Soukka, Tero; Vosch, Tom André Jos

Published in:
Chemistry: A European Journal

DOI:
10.1002/chem.201801962

Publication date:
2018

Document version
Publisher's PDF, also known as Version of record

ChemPubSoc Europe

DOI: 10.1002/chem.201801962

CHEMISTRY A European Journal Communication

Nanotechnology | *Very Important Paper*

VIP Upconversion Cross-Correlation Spectroscopy of a Sandwich Immunoassay

Satu Lahtinen[+],[a] Stefan Krause[+],[b] Riikka Arppe,[b] Tero Soukka,*[a] and Tom Vosch*[b]

Abstract: Fluorescence correlation and cross-correlation spectroscopy (FCS/FCCS) have enabled biologists to study processes of transport, binding, and enzymatic reactions in living cells. However, applying FCS and FCCS to samples such as whole blood and plasma is complicated as the fluorescence bursts of diffusing labels can be swamped by strong autofluorescence. Here we present cross-correlation spectroscopy based on two upconversion nanoparticles emitting at different wavelengths on the anti-Stokes side of a single excitation laser. This upconversion cross-correlation spectroscopy (UCCS) approach allows us to completely remove all Stokes shifted autofluorescence background in biological material such as plasma. As a proof of concept, we evaluate the applicability of UCCS to a homogeneous sandwich immunoassay for thyroid stimulating hormone measured in buffer solution and in plasma.

Throughout the past fifty years, fluorescence (cross-)correlation spectroscopy (FCS/FCCS) has been established as an important tool in life sciences.[1] It enabled numerous in vitro and in vivo studies of membrane diffusion, enzymatic activities, protein–protein interactions and others.[2] Since FCS/FCCS is based on measuring fluorescence fluctuations in a diffraction-limited volume of a few femtoliters, it allows detecting dye concentrations down to the single molecule level (usually sub-nanomolar).

However, when it comes to strong autofluorescent samples, for example, blood or plasma, the FCS/FCCS signal of sub-nanomolar probe concentrations might vanish in the spectrally overlapping autofluorescence background. In addition, conventional FCS and FCCS labels, such as fluorescent dyes and proteins, are also vulnerable to photobleaching and fluorescence intermittency, which can disturb the FCS/FCCS signal.[3] Here we present a correlation spectroscopy method based on upconversion emission of lanthanide-doped nanoparticles.[4] Upconversion nanoparticles (UCNPs) have the ability to convert low energy near-infrared (NIR) light into emission at ultraviolet or visible wavelengths due to a sequential absorption of two or more photons.[4b] Because the Stokes-shifted autofluorescence occurs at NIR wavelengths, detecting the anti-Stokes shifted upconverted emission allows us to easily remove the entire autofluorescence background. Moreover, UCNPs exhibit excellent photostability, lanthanide ion-specific narrow band emission and low cytotoxicity.[5] A minor drawback accompanying UCNP application is the low quantum yield which, however, can be compensated by higher excitation power and tailoring of the particle size which affects both, brightness and average diffusion time through the laser focus.[6]

We demonstrate the potential of our approach by applying upconversion cross-correlation spectroscopy (UCCS) to an immunoassay for thyroid stimulating hormone (TSH). The assay is based on anti-TSH antibody-conjugated green ($NaYF_4$:Yb^{3+}, Er^{3+}) and blue ($NaYF_4$:Yb^{3+},Tm^{3+})-emitting UCNPs measured at spectrally separated detection channels. Thereby, the cross-correlation amplitude of the two channels serves as an indicator for the formation of the sandwich complex between the two nanoparticles and the analyte.

The $NaYF_4$:Yb^{3+},Tm^{3+} and $NaYF_4$:Yb^{3+},Er^{3+} UCNPs used in the study were 30 nm and 26 nm in average dimension, respectively, according to TEM images (Figure S1, Supporting Information). The principle of the UCCS TSH sandwich immunoassay is illustrated in Scheme 1. The TSH is bound by the blue emitting $NaYF_4$:Yb^{3+},Tm^{3+} and the green emitting $NaYF_4$:Yb^{3+}, Er^{3+} UCNPs which are conjugated with antibodies recognizing different epitopes of TSH, thus forming a sandwich complex. The immunoassay is a separation-free homogeneous assay and therefore no washing steps are needed. During the UCCS measurement the binding of the TSH analyte is recognized from the simultaneous emission of blue and green light upon 977 nm laser excitation. The unbound single particles only emit at their specific wavelength being recognized in either the Er^{3+} (green) or Tm^{3+} (blue) detection channel.

We measured photon macro times (elapsed time since the start of the measurement) to construct intensity time traces by binning the detected photons in time intervals of 2 ms as can be seen in Figure 1a for the mixture of $NaYF_4$:Yb^{3+},Tm^{3+} and

[a] *S. Lahtinen,[+] Prof. Dr. T. Soukka*
Department of Biotechnology, University of Turku
Medisiina D6, Kiinamyllynkatu 10, 20520 Turku (Finland)
E-mail: tejoso@utu.fi

[b] *Dr. S. Krause,[+] Dr. R. Arppe, Prof. Dr. T. Vosch*
Nano-Science Center, Department of Chemistry, University of Copenhagen
Universitetsparken 5, 2100 Copenhagen (Denmark)
E-mail: tom@chem.ku.dk

[+] *These authors contributed equally to this work.*

Supporting information and the ORCID number(s) for the author(s) of this article can be found under https://doi.org/10.1002/chem.201801962.

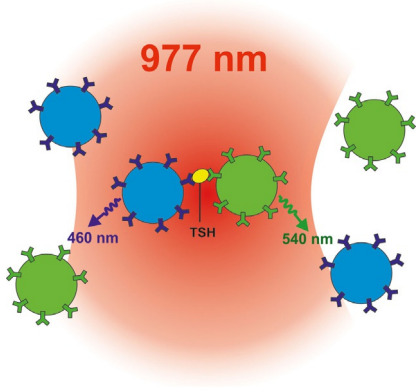

Scheme 1. Principle of the UCCS TSH sandwich immunoassay. The bound TSH is recognized by the simultaneous diffusion of $NaYF_4$:Yb^{3+},Tm^{3+} (blue) and $NaYF_4$:Yb^{3+},Er^{3+} (green) nanoparticles through the 977 nm laser focal volume resulting in coincident emission of both species.

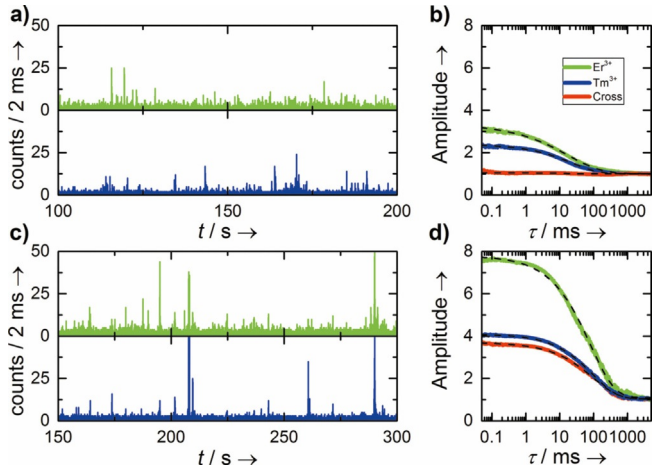

Figure 1. a) Example of a time trace for a mixture of NaYF4:Yb^{3+},Er^{3+} (green) and NaYF4:Yb^{3+},Tm^{3+} (blue) antibody-conjugated UCNPs without TSH. The traces were binned to 2 ms. b) AC and CC curves calculated from the data in a). c) Example of a time trace of a similar mixture of UCNPs as presented in a) containing 2880 mIU L^{-1} TSH. The traces were binned to 2 ms. d) AC and CC curves calculated from the data in c).

$NaYF_4$:Yb^{3+},Er^{3+} antibody conjugated UCNPs in buffer without TSH analyte.[7] It is obvious from Figure 1a and the cross-correlation amplitude A_{CC} in Figure 1b that the two detection channels for Er^{3+} and Tm^{3+} do not show any simultaneous fluorescence bursts. Adding 2880 mIU L^{-1} of the TSH analyte to the UCNP mixture in buffer results in binding of the $NaYF_4$:Yb^{3+}, Tm^{3+} and $NaYF_4$:Yb^{3+},Er^{3+} particles to the analyte and in fluorescence bursts being detected simultaneously in both channels as shown in Figure 1c, for example, at around 210 s and 290 s. This can also be seen from the increased A_{CC} in Figure 1d versus b. An observed issue in the UCCS-based sandwich immunoassay was the formation of large UCNP aggregates. These aggregates can emerge either from UCNP-aggregation without TSH being involved (due to non-specific interactions between the UCNPs) or from TSH induced bridging of more than two UCNPs (specific binding). In order to try and remedy this issue, large intensity bursts above 100 counts per 2 ms were removed from the dataset before auto- (AC) and cross-correlation (CC) functions were calculated by applying a multiple-tau algorithm with progressive binning.[7] An example of such large intensity spikes in the dataset and their effect on the CC function can be seen in Figure S2 in the Supporting Information. For analysis of the binding events between the antibody-conjugated $NaYF_4$:Yb^{3+},Tm^{3+} and $NaYF_4$:Yb^{3+},Er^{3+} UCNPs, we are most of all interested in A_{CC}. This amplitude was extracted by fitting a stretched exponential with the correlation time τ_S and the stretching exponent β in Equation (1) to the data.

$$A(\tau) = A_{CC} \cdot \exp(-\tau/\tau_S)^{\beta} + 1 \quad (1)$$

Application of a stretched exponential function mainly takes into account dimer/multimer formation and size polydispersity of the UCNPs. We like to mention that in standard FCS/FCCS applications based on dye molecules, a three-dimensional diffusion model is more appropriate.[8] However, in the present case we are not facing diffusion of a chemically well-defined molecule but rather diffusion of polydisperse nano-particles with a probability of forming aggregates. Figure 1b and d display examples of AC and CC functions for the mixtures with 0 and 2880 mIU L^{-1} TSH analyte. Examination of the CC function (red) reveals amplitudes of 0.043 (0 mIU L^{-1} TSH) and 2.66 (2880 mIU L^{-1} TSH). The increased A_{CC} results from binding of the antibody conjugated Er^{3+} and Tm^{3+} doped UCNPs by the TSH analyte which then diffuse as a sandwich complex through the laser focus and emit simultaneously in both detection channels. From this we can conclude that A_{CC} depends strongly on the TSH concentration. On the other hand, the auto-correlation amplitudes A_{AC} remain at least similar as expected for a constant concentration of both UCNP species (final concentration 0.0118 mg mL^{-1} in measurement volume for $NaYF_4$:Yb^{3+},Tm^{3+} and $NaYF_4$:Yb^{3+},Er^{3+}. See also Figure S3 in the Supporting Information). The variations in A_{AC} for $NaYF_4$:Yb^{3+},Er^{3+} and $NaYF_4$:Yb^{3+},Tm^{3+} in Figure 1b and d can be explained by statistical fluctuations for this short example trace. However, averaging over about five to ten, 300 s long intensity traces for a distinct concentration yields similar A_{AC} values (see Figure S3). We like to point out that deviations in the simultaneous emission of the two linked UCNPs could occur due to differences in the rates of their inherent excitation energy-migration dynamics and relatively long apparent luminescent lifetimes in the range of a few hundred microseconds.[9] This could be problematic if the diffusion times for passing the diffraction limited spot were on the same timescale of the luminescence decay time. From theoretical calculations we expect a diffusion time of 15.4 ms (see calculations in Figure S4). In order to compare this value to our experimental data we have to apply the above mentioned three-dimensional diffusion model.[8] However, the previously described particle polydispersity and aggregation prevents us to simply apply a one-component three-dimensional diffusion model but requires at least two components as can be seen from the fitting residuals in Figure S5. We attribute the first and faster diffusion component to the desired translational diffusion of either

single UCNPs or sandwich complexes consisting of only two UCNPs bound by a TSH analyte. This first component yields an average value of 13.5 ms (from the AC fitting) in good agreement with the theoretical value for the diffusion of single UCNPs and 27 ms (from the CC fitting) for the diffusion of the TSH bound sandwich structure (see Figure S6). The second and slower diffusion component is associated with larger aggregates being formed. The contribution of the second amplitude to the overall A_{AC} and A_{CC} is limited, as can be seen from comparing Figure 2 with Figure S6.

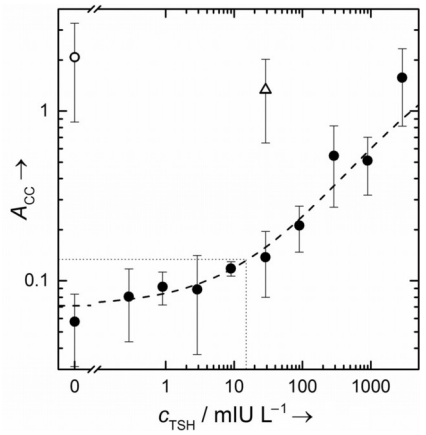

Figure 2. Standard curve for the TSH immunoassay. The curve was fitted with a four-parameter logistic function. The dashed lines represent the limit of detection of the curve. The open circle and open triangle represent A_{CC} values for measurements in normal unspiked (plotted at 0 mIU L^{-1}) and spiked (plotted at 28.8 mIU L^{-1}) plasma. The intrinsic amount of TSH in the plasma was not determined and hence not added to the spiked and unspiked amount plotted in the graph. The amplitudes A_{CC} were extracted by fitting a stretched exponential function to the experimental data. The A_{CC} values and their error bars represent the averaged amplitudes and standard deviations of at least five replicate measurements with a length of 300 s each.

A standard curve for the UCCS TSH sandwich immunoassay calculated from A_{CC} is shown in Figure 2. A_{CC} increases when both $NaYF_4$:Yb^{3+},Tm^{3+} and $NaYF_4$:Yb^{3+},Er^{3+} UCNPs are bound to TSH simultaneously. Figure 2 shows a clear dependency of the A_{CC} versus TSH concentration with a linear increase between 28.8–2880 mIU L^{-1} of TSH in the double logarithmic plot. The limit of detection (LoD) was calculated by adding three times the standard deviation to the average A_{CC} of the blank (0 mIU L^{-1} TSH) sample. The standard curve was fitted with a four-parameter logistic function of the form $A_{CC}=A_1+(A_1-A_2)/(1+(c_{TSH}/c_0)^p)$ with fitting parameters $A_1=0.07\pm0.02$, $A_2=2.77\pm0.3$, $c_0=(12\pm8)\times10^3$ mIU L^{-1} and $p=0.56\pm0.08$.[10] The LoD for TSH in the binding reaction was 15 mIU L^{-1} (14 mIU L^{-1} for the fast component of the two-component three-dimensional diffusion model as shown in Figure S6). For the UCCS measurements, the actual reaction mixture was diluted 33 times. The undiluted values were used to create the standard curve in Figure 2. The normal range of TSH in serum is 0.3–5.0 mIU L^{-1} and thus, the LoD for our proof of principle sandwich immunoassay reaction is not able to detect normal TSH values in human serum.[11] However, there is significant room for improvement in the sandwich immunoassay by optimizing the surface chemistry of the UCNPs in order to prevent aggregation. Additionally, the presented proof of concept was a separation-free homogeneous assay with a short incubation time of 30 min and thus, cannot be compared to the highly sensitive heterogeneous assays with longer incubation times and washing of extra reagents reaching LoD values down to 60×10^{-6} mIU L^{-1}.[12]

The major issue limiting the LoD is the UCNP aggregation. The nanoparticles can aggregate during the surface modification steps and they can bind non-specifically with each other during the immunoassay. The high luminescence bursts of aggregates influence the CC function and cause strong variations of the amplitudes even after obviously too high bursts are removed.[13] Therefore, the monodispersity of the UCNPs is of high importance but challenging to achieve with any nanoparticles.[14] The LoD could also be lowered by optimizing the UCNP concentration. In the current immunoassay, the molar amount of the individual UCNPs was estimated to be two times higher than the highest TSH concentration tested. The UCNP conjugates were intended to have more than one antibody attached but the exact number of antibodies per UCNP was not determined. The nanoparticle concentration has to be larger than the concentration of the analyte in order to reduce bridging of multiple nanoparticles (cross-linking, multimer formation). These high nanoparticle concentrations increase their non-specific aggregation probability and reduce the A_{AC} and A_{CC} (Figure S7, Supporting Information). By optimizing the nanoparticle concentration for lower TSH values the LoD could be improved. In addition, increasing the measurement time from five minutes per trace to longer times would also improve statistics and therefore sensitivity. However, the UCNPs had a tendency to stick to the glass coverslip over time and hence effectively lower the concentration of UCNPs and linked UCNPs over time. This could be prevented by coating the glass coverslips with bovine serum albumin (BSA), or by using an uncleaned coverslip where the droplet would have a smaller contact area with the glass surface.

Despite the aforementioned issues that still require optimization, the UCCS sandwich immunoassay was tested with normal human plasma and plasma spiked with 28.8 mIU L^{-1} of TSH (Figure 3). In the spiked plasma the $NaYF_4$:Yb^{3+},Tm^{3+} and $NaYF_4$:Yb^{3+},Er^{3+} UCNPs have highly correlated time traces and large A_{CC} values (see open triangle in Figure 2), but even in the normal plasma (with a low intrinsic concentration of THS; see open circle in Figure 2) the A_{CC} value reached a similar magnitude within the accuracy of our measurement. This can be explained with the increased non-specific binding and aggregation of UCNPs in plasma due its complex composition. The lack of autofluorescence in the UCCS measurements was demonstrated by recording emission spectra of UCNPs in the presence of plasma when excited at 977 nm and 458 nm (used for common fluorescence labels), see Figure 3c. The 458 nm excitation exhibits strong autofluorescence, which would swamp the fluorescence of all standard FCS/FCCS labels at sub-nanomolar concentrations. With 977 nm NIR excitation no autofluorescence was detected on the anti-Stokes side of the excitation.

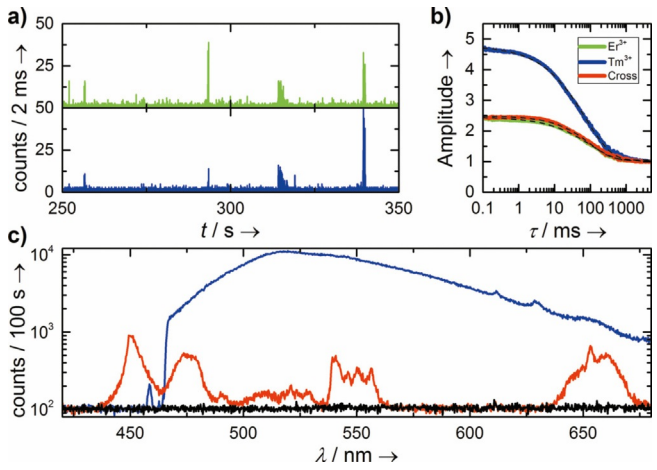

Figure 3. a) Example time trace of a plasma sample spiked with 28.8 mIU L^{-1} of TSH for Er^{3+} (green detection channel) and Tm^{3+} (blue detection channel). The traces were binned to 2 ms. The spiked plasma sample was prepared the same way as the standard TSH-dilutions, except by using a plasma pool collected from healthy volunteers in place of TSA-BSA. The final plasma and TSH concentrations in the reaction were 20% and 28.8 mIU L^{-1}, respectively. The intrinsic amount of TSH in the plasma was not determined and not included in the TSH concentration. b) Auto- and cross- correlation curves calculated from the data belonging to a). c) Emission spectra acquired in blood plasma with (blue, red curve) and without (black curve) UCNPs. The blue curve was acquired with a 458 nm long pass filter, 458 nm excitation wavelength and an excitation intensity of about 6.7 kW cm^{-2}. The red and black curves were acquired with 977 nm excitation wavelength and an excitation intensity of about 1.8 MW cm^{-2}. All spectra were recorded with an exposure time of 100 s.

The latter experiment shows the large potential of UCCS, since it gives no background in the native plasma sample.

In this study, UCCS was presented and its applicability was evaluated using a homogeneous TSH sandwich immunoassay. In the assay, simultaneous emission of two differently emitting UCNPs was detected upon sandwich formation with the TSH analyte. Upconversion emission detection enabled measurements completely free from autofluorescence in buffer and in plasma, but the detectability of TSH in plasma was degraded by the aggregation of UCNPs. The study, however, demonstrates the use of the UCNP labels for UCCS and the great potential of UCCS for samples and environments challenging for conventional FCCS measurements. In addition, our work on UCCS constitutes a proof of concept which is not restricted to in vitro immunoassays, but has potential also to in vivo applications, for example, in cells. Improvements in particle surface chemistry to prevent aggregation and non-specific interactions would reduce the current limitations of UCCS highlighted in this article.

Experimental Section

Materials. $NaYF_4$:Yb^{3+},Er^{3+} (X_{Yb} = 0.17, X_{Er} = 0.03) and $NaYF_4$:Yb^{3+},Tm^{3+} (X_{Yb} = 0.2, X_{Tm} = 0.005) UCNPs were synthesized in organic oils.[15] Poly(acrylic acid) (PAA, M = 2000 g mol^{-1}, Sigma–Aldrich) was used for UCNP coating. Monoclonal antibody (Mab) clones 5404 and 5409 specific for human TSH were purchased from Medix Biochemica (Espoo, Finland). Human TSH was from Scripp Laboratories (San Diego, CA). *N*-hydroxysuccinimide (sulfo-NHS) and *N*-(3-dimethylaminopropyl)-*N*′-ethylcarbodiimide (EDC) were from Sigma–Aldrich (St. Louis, MO). Bovine serum albumin (BSA) was purchased from Bioreba. Assay buffer was from Kaivogen (Kaivogen Assay Buffer, Turku Finland).

Upconverting nanoparticle surface chemistry. After the synthesis, the oleic acid-covered UCNPs are insoluble in water and do not have any functional groups. Therefore, after removing the oleic acid the $NaYF_4$:Yb^{3+},Er^{3+} and $NaYF_4$:Yb^{3+},Tm^{3+} UCNPs were coated with PAA.[16] After the PAA coating, the green-emitting $NaYF_4$:Yb^{3+},Er^{3+} UCNPs were conjugated to Mab-5409 antibody and the blue-emitting $NaYF_4$:Yb^{3+},Tm^{3+} UCNPs to Mab-5404. The Mab 5404 and Mab 5409 recognize two different epitopes on human TSH and therefore, enable simultaneous binding of green and blue emitting UCNPs to the same TSH molecule. The Mab conjugation to UCNPs was performed according to protocol described previously using standard EDC/sulfo-NHS chemistry.[17] In the reaction, 0.167 mg of Mab was used for 2 mg of UCNPs in a 250 μL volume.

Immunoassay. The final volume of the TSH immunoassay was 30 μL comprising the combined volume of 17.8 μL of $NaYF_4$:Yb^{3+}, Er^{3+} and $NaYF_4$:Yb^{3+},Tm^{3+} Mab conjugated UCNPs in assay buffer in final concentrations of 0.39 mg mL^{-1} and 10 μL TSH in tris-saline-azide buffer (TSA) supplemented with 75 g L^{-1} BSA (further referred to as TSA-BSA) in final concentrations of 0–2880 mIU·L^{-1}. The activity of TSH was 10.8 IU mg^{-1} as provided from the manufacturer. The total volume of the sample was adjusted to 30 μl with assay buffer. The final TSA-BSA amount in the sample was 20%, the remaining 80% was assay buffer. The antibodies were enabled to bind with TSH for 30 minutes and then a 33-fold dilution was made to assay buffer/D_2O (1/10) for the UCCS, giving final UCNP concentration of 0.0118 mg mL^{-1} in the measurement volume. The dilution contained 10% of assay buffer to prevent aggregation after diluting the nanoparticles. Otherwise the UCNPs were diluted to D_2O to enhance the lanthanide emission intensity and prevent sample heating due to water absorption by the laser.[18]

A plasma pool collected from healthy volunteers was spiked with TSH so that the final concentrations of plasma and added TSH in the reaction were 20% and 28.8 mIU·L^{-1}, respectively. Also non-spiked plasma was used. The spiked plasma was added in 10 μl volume to the mixture of $NaYF_4$:Yb^{3+},Er^{3+} and $NaYF_4$:Yb^{3+},Tm^{3+} Mab conjugated UCNPs in assay buffer, and the volume was adjusted to 30 μl with assay buffer. The immune complex was allowed to form for 30 minutes before diluting as mentioned above.

Upconversion Cross-Correlation Spectroscopy. UCCS time traces were acquired with a home-build confocal microscope.[19] The setup is shown in Figure S8 in the Supporting Information along with all optical components. We used the output of a continuous wave Ti-sapphire laser (3900S Spectra-Physics) which was tuned to an emission wavelength of 977 nm. The laser emission was cleaned up by a 815 nm long pass filter (HQ815LP) and then reflected by a 30:70 beam splitter (XF122 Omega Optical) into an oil immersion objective (Olympus, UPlanSApo 100× NA = 1.4) focusing the laser on a spot with a 1/e^2—beam radius of about 840 nm (see Figure S4). The fluorescence signal was collected with the same objective. The laser light was blocked by a 950 nm short pass filter (Semrock FF01-950/SP-25) and a 700 nm short pass filter (Chroma, ET700SP-2P8). The upconversion signal was separated into two spectral channels for detection of the emission of either the erbium or thulium doped UCNPs only by a 488 nm dichroic mirror. Further spectral filtering was achieved with a band pass filter (RPB 520–560) and a long pass filter (BLP01-532R-25) in the erbium channel and a band pass filter (FF01-473/10–25 at 54° angle of in-

cidence) and a short pass filter (500SP) in the thulium channel transmitting only the spectral ranges shown in Figure S8. The signals were then detected by avalanche photodiodes (PerkinElmer CD3226) connected to a single photon counting module (Becker & Hickl SPC-830). The higher quantum yield of Er^{3+} doped UCNPs in comparison to Tm^{3+} doped UCNPs was taken into account by a 0.7 neutral density filter in front of the Er^{3+} detecting avalanche photodiode.[6] Recording of spectra was achieved by sending the fluorescence signal to a liquid nitrogen cooled spectrograph (Princeton Instruments SPEC-10:100B/LN eXcelon CCD camera, SP 2356 spectrometer, 300 grooves mm^{-1}). Data was analyzed with self-written Matlab algorithms.

Acknowledgements

We gratefully acknowledge financial support from the "Center for Synthetic Biology" at Copenhagen University funded by the UNIK research initiative of the Danish Ministry of Science, Technology and Innovation (Grant 09–065274), bioSYNergy, University of Copenhagen's Excellence Programme for Interdisciplinary Research, the Villum Foundation (Project number VKR023115), the Carlsberg Foundation (CF14-0388), the Danish Council of Independent Research (Project number DFF-7014-00027) and Tekes, the Finnish Funding Agency for Innovation and the Doctoral Programme in Molecular Life Sciences.

Conflict of interest

The authors declare no conflict of interest.

Keywords: Fluorescence Correlation Spectroscopy · Immunoassays · Lanthanides · Nanochemistry · Upconversion

[1] a) E. L. Elson, D. Magde, *Biopolymers* **1974**, *13*, 1–27; b) E. Haustein, P. Schwille, *Annu. Rev. Bioph. Biom.* **2007**, *36*, 151–169; c) O. Krichevsky, B. Grégoire, *Rep. Prog. Phys.* **2002**, *65*, 251.

[2] a) S. T. Hess, S. Huang, A. A. Heikal, W. W. Webb, *Biochemistry* **2002**, *41*, 697–705; b) P. Schwille, J. Korlach, W. W. Webb, *Cytometry* **1999**, *36*, 176–182; c) S. Weiss, *Science* **1999**, *283*, 1676–1683.

[3] a) W. P. Ambrose, P. M. Goodwin, J. C. Martin, R. A. Keller, *Phys. Rev. Lett.* **1994**, *72*, 160–163; b) C. Eggeling, J. Widengren, R. Rigler, C. A. M. Seidel, *Anal. Chem.* **1998**, *70*, 2651–2659.

[4] a) D. J. Gargas, E. M. Chan, A. D. Ostrowski, S. Aloni, M. V. P. Altoe, E. S. Barnard, B. Sanii, J. J. Urban, D. J. Milliron, B. E. Cohen, P. J. Schuck, *Nat. Nanotechnol.* **2014**, *9*, 300; b) M. Haase, H. Schäfer, *Angew. Chem. Int. Ed.* **2011**, *50*, 5808–5829; *Angew. Chem.* **2011**, *123*, 5928–5950.

[5] F. Wang, X. Liu, *Chem. Soc. Rev.* **2009**, *38*, 976–989.

[6] a) C. Würth, M. Kaiser, S. Wilhelm, B. Grauel, T. Hirsch, U. Resch-Genger, *Nanoscale* **2017**, *9*, 4283–4294; b) C. T. Xu, P. Svenmarker, H. Liu, X. Wu, M. E. Messing, L. R. Wallenberg, S. Andersson-Engels, *ACS Nano* **2012**, *6*, 4788–4795; c) C. T. Xu, Q. Zhan, H. Liu, G. Somesfalean, J. Qian, S. He, S. Andersson-Engels, *Laser Photonics Rev.* **2013**, *7*, 663–697.

[7] W. Becker in *Advanced Time-Correlated Single Photon Counting Techniques, Vol. 81*, Springer Science & Business Media, **2005**, pp. 180.

[8] a) K. Bacia, P. Schwille, *Nat. Protoc.* **2007**, *2*, 2842; b) J. Ries, P. Schwille, *BioEssays* **2012**, *34*, 361–368; c) S. Aragón, R. Pecora, *J. Chem. Phys.* **1976**, *64*, 1791–1803.

[9] a) C. F. Gainer, G. S. Joshua, C. R. De Silva, M. Romanowski, *J. Mater. Chem.* **2011**, *21*, 18530–18533; b) E. Lee, M. Jung, Y. Han, G. Lee, K. Shin, H. Lee, K. T. Lee, *J. Phys. Chem. C* **2017**, *121*, 21073–21079.

[10] K. L. Cox, V. Devanarayan, A. Kriauciunas, J. Manetta, C. Montrose, S. Sittampalam in *Assay Guidance Manual, Eli Lilly & Company and the National Center for Advancing Translational Sciences, Internet, May 1, 2012*; Last Update: December 24, **2014**.

[11] L. M. Demers, C. A. Spencer, *Clin. Endocrinol.* **2003**, *58*, 138–140.

[12] a) Y. Zhou, X. Xia, Y. Xu, W. Ke, W. Yang, Q. Li, *Anal. Chim. Acta* **2012**, *722*, 95–99; b) T. Näreoja, J. M. Rosenholm, U. Lamminmäki, P. E. Hänninen, *Anal. Bioanal. Chem.* **2017**, *409*, 3407–3416.

[13] a) A. E. Miller, C. W. Hollars, S. M. Lane, T. A. Laurence, *Anal. Chem.* **2009**, *81*, 5614–5622; b) J. Wang, X. Huang, H. Liu, C. Dong, J. Ren, *Anal. Chem.* **2017**, *89*, 5230–5237.

[14] a) F. Wang, D. Banerjee, Y. Liu, X. Chen, X. Liu, *Analyst* **2010**, *135*, 1839–1854; b) H. S. Mader, P. Kele, S. M. Saleh, O. S. Wolfbeis, *Curr. Opin. Chem. Biol.* **2010**, *14*, 582–596.

[15] E. Palo, M. Tuomisto, I. Hyppänen, H. C. Swart, J. Hölsä, T. Soukka, M. Lastusaari, *J. Lumin.* **2017**, *185*, 125–131.

[16] N. Sirkka, A. Lyytikäinen, T. Savukoski, T. Soukka, *Anal. Chim. Acta* **2016**, *925*, 82–87.

[17] K. Kuningas, T. Rantanen, T. Ukonaho, T. Lövgren, T. Soukka, *Anal. Chem.* **2005**, *77*, 7348–7355.

[18] Q. Zhan, J. Qian, H. Liang, G. Somesfalean, D. Wang, S. He, Z. Zhang, S. Andersson-Engels, *ACS Nano* **2011**, *5*, 3744–3757.

[19] Z. Liao, E. N. Hooley, L. Chen, S. Stappert, K. Müllen, T. Vosch, *J. Am. Chem. Soc.* **2013**, *135*, 19180–19185.

Manuscript received: April 19, 2018

Accepted manuscript online: May 3, 2018

Version of record online: June 7, 2018

